

COMPARISON OF LOCAL RADIATION BOUNDARY CONDITIONS FOR THE SCALAR HELMHOLTZ EQUATION WITH GENERAL BOUNDARY SHAPES†

Douglas B. Meade*, G. William Slade♣, Andrew F. Peterson♣, and Kevin J. Webb♣

* Department of Mathematics, University of South Carolina, Columbia, SC 29208

♣ School of Electrical Engineering, Purdue University, West Lafayette, IN 47907

♣ School of Electrical Engineering, Georgia Institute of Technology, Atlanta, GA 30332

Abstract — The relative accuracy of several local radiation boundary conditions based on the second-order Bayliss–Turkel condition are evaluated. These boundary conditions permit the approximate solution of the scalar Helmholtz equation in an infinite domain using traditional finite element and finite difference techniques. Unlike the standard Bayliss–Turkel condition, the generalizations considered here are applicable to non-circular solution domains. The accuracy of these conditions are investigated for elliptical and linear/circular boundaries.

I. Introduction

When solving the scalar Helmholtz equation in unbounded regions, a radiation boundary condition (RBC) must be imposed to obtain a unique solution. Efficient numerical solution procedures for scattering problems necessitate the imposition of an RBC as close as possible to the scatterer. In order to maintain the desirable sparse characteristics of a differential equation formulation, a local RBC is often employed. Bayliss and Turkel (BT) [1], [2] have proposed RBCs which approximately absorb outgoing waves over a circular or spherical boundary. A wide variety of other local RBCs have been proposed [3, 4], and are usually similar in form to the BT expressions. In this article we consider the extension of the second-order BT RBC to non-circular boundaries. A conformal RBC can be used to limit the extent of the computational domain and provide a more efficient numerical analysis.

The adaptation of the second-order BT RBC to general shapes is straightforward. The main ingredient is a change of variable from a cylindrical (ρ, ϕ) to a local (n, t) coordinate system, where n and t are the coordinates normal and tangential to the boundary,

† This work was supported in part by the Semiconductor Research Corporation under contract 92-DJ-211.

respectively. The mixed derivative in the resulting RBC complicates the use of this RBC for a non-circular boundary. Moore et al. [3], Khebir et al. [5] and Janaswamy [6] have proposed approximations which avoid the cross-derivative term. Here we present the exact curvilinear form of the second-order Bayliss-Turkel radiation boundary condition and evaluate several proposed approximations. We note that other conformable radiation conditions have been proposed [7-9]. The RBC presented by Ma is applicable to a substantially different formulation of the scattering problem, while those proposed by Jones and Kriegsmann [8] and Lee et al. [9] are not based on the BT condition and therefore differ from those considered here.

II. The Bayliss–Turkel Boundary Condition

Consider the two-dimensional Helmholtz equation with wave-number k

$$\nabla^2 u + k^2 u = 0 \quad (1)$$

in an exterior domain. The N th order BT RBC forces the solution to agree with the first $2N$ terms of the asymptotic expansion

$$u = \frac{e^{-jk\rho}}{\sqrt{k\rho}} \sum_{n=0}^{\infty} a_n(\phi)(k\rho)^{-n}, \quad (2)$$

with a resulting error of $O(\rho^{-2N-1/2})$. The expression for u in (2) is an approximation of the true scattered field [10], and is not valid close to the scatterer. The first- and second-order BT boundary conditions can be expressed as

$$u_\rho = \alpha_i(\rho)u + \beta_i(\rho)u_{\phi\phi} \quad (3)$$

where

$$\alpha_1(\rho) = -(jk + \frac{1}{2\rho}), \quad \beta_1 = 0 \quad (4a)$$

$$\alpha_2(\rho) = \frac{-jk - \frac{3}{2\rho} + \frac{j^3}{8k\rho^2}}{1 - \frac{j}{k\rho}}, \quad \beta_2 = -\frac{\frac{j}{2k\rho^2}}{1 - \frac{j}{k\rho}} \quad (4b)$$

III. Generalized Radiation Boundary Condition for Curved Boundaries

A radiation boundary condition for a non-circular boundary can be derived from the Bayliss–Turkel RBC, (3) with (4b), and a parametric description of the artificial boundary,

$\partial\Omega$. Let $\partial\Omega$ be parameterized by arclength, t , as $\partial\Omega = \{(X(t), Y(t)) : 0 \leq t \leq L\}$ where L is the perimeter of the boundary curve. A new coordinate system for the exterior region can be defined in terms of t , the arclength, and n , the distance from $\partial\Omega$ as measured along a normal vector (see Figure 1). That is,

$$\begin{aligned}x &= X(t) + nY'(t), \\y &= Y(t) - nX'(t)\end{aligned}$$

The Jacobian of this transformation is $Q(n, t) = 1 + n\kappa(t)$, where $\kappa \geq 0$ is the curvature of $\partial\Omega$. When $\partial\Omega$ is convex, i.e. $\kappa > 0$, this coordinate system is global in the exterior of the artificial boundary.

A direct change of coordinates between polar coordinates and (t, n) coordinates is obtained by the composition of the standard change of coordinates between polar and Cartesian coordinates with the above conversion from Cartesian coordinates to (t, n) -space. Thus

$$\begin{aligned}u_n &= \frac{\partial\rho}{\partial n}u_\rho + \frac{\partial\phi}{\partial n}u_\phi \\ &= \alpha_2 \frac{\partial\rho}{\partial n}u + \frac{\partial\phi}{\partial n}u_\phi + \beta_2 \frac{\partial\rho}{\partial n}u_{\phi\phi}\end{aligned}\tag{5}$$

The final step is to express the derivatives on the right-hand side of (5) in terms of tangential and normal derivatives on $\partial\Omega$. The composite coordinate transformation yields

$$u_\phi = \frac{\partial t}{\partial\phi}u_t + \frac{\partial n}{\partial\phi}u_n\tag{6a}$$

and

$$u_{\phi\phi} = \left(\frac{\partial t}{\partial\phi}\right)^2 u_{tt} + 2\frac{\partial t}{\partial\phi}\frac{\partial n}{\partial\phi}u_{tn} + \left(\frac{\partial n}{\partial\phi}\right)^2 u_{nn} + \frac{\partial^2 t}{\partial\phi^2}u_t + \frac{\partial^2 n}{\partial\phi^2}u_n.\tag{6b}$$

From (6a) and (6b) it is seen that (5) leads to an RBC in which u_n is expressed in terms of u , u_t , u_{tt} , u_{tn} , and u_{nn} .

The Helmholtz equation (1) can be used to express the second normal derivative in terms of only tangential quantities: u , u_t , and u_{tt} . The curvilinear form of the Helmholtz equation is

$$\frac{1}{Q^2}u_{tt} - \frac{n\kappa'}{Q^3}u_t + u_{nn} + \frac{\kappa}{Q}u_n + k^2u = 0.\tag{7}$$

The resulting radiation boundary condition is

$$0 = Au + Bu_t + Cu_n + Du_{tt} + Eu_{tn}\tag{8}$$

where‡

$$\begin{aligned}
A &= \alpha_2 - k^2 \beta_2 \left(\frac{\partial n}{\partial \phi} \right)^2 \\
B &= - \frac{\partial t}{\partial \rho} + \beta_2 \frac{\partial^2 t}{\partial \phi^2} \\
C &= - \frac{\partial n}{\partial \rho} + \beta_2 \left(\frac{\partial^2 n}{\partial \phi^2} - \kappa \left(\frac{\partial n}{\partial \phi} \right)^2 \right) \\
D &= \beta_2 \left(\left(\frac{\partial t}{\partial \phi} \right)^2 - \left(\frac{\partial n}{\partial \phi} \right)^2 \right) \\
E &= 2\beta_2 \frac{\partial t}{\partial \phi} \frac{\partial n}{\partial \phi}.
\end{aligned}$$

We emphasize that (8) is an *exact* extension of the second-order BT RBC, (3) with (4b), to a non-circular artificial boundary; no earlier work gives an exact extension.

It is not possible to express u_{tn} in terms of the remaining terms in (8). The presence of u_{tn} in (8) is problematic for two reasons: (i) the RBC involves field data off the boundary, in contrast to a classical boundary condition, and (ii) the mixed derivative unduly complicates a finite element implementation. Therefore, various authors have proposed ways of avoiding the u_{tn} term. Three different approximations of this term will be investigated. In each case the resulting RBC is of the form

$$0 = \tilde{A}u + \tilde{B}u_t + \tilde{C}u_n + \tilde{D}u_{tt}. \quad (9)$$

The simplest approximation is to assume that the mixed derivative of the solution is “small,” so that the offending term can be ignored [3, 5]. This yields (9) with coefficients

$$\tilde{A} = A, \quad \tilde{B} = B, \quad \tilde{C} = C, \quad \tilde{D} = D. \quad (10)$$

A second approximation to u_{tn} can be obtained by taking a tangential derivative of the first-order BT RBC,§ i.e. (3) with (4a). Inserting the resulting expression for the

‡ To reach this form it is necessary to assume that $\frac{\partial \rho}{\partial n} \neq 0$ and to notice that

$$1 = \frac{\partial n}{\partial \rho} \frac{\partial \rho}{\partial n} + \frac{\partial n}{\partial \phi} \frac{\partial \phi}{\partial n} \quad \text{and} \quad 0 = \frac{\partial t}{\partial \rho} \frac{\partial \rho}{\partial n} + \frac{\partial t}{\partial \phi} \frac{\partial \phi}{\partial n}.$$

§ Janaswamy [6] uses the first-order BT RBC in a similar manner to obtain good results with a boundary element method for the Helmholtz equation.

mixed derivative into (8) leads to an RBC in the form of (9) with coefficients

$$\tilde{A} = A + \frac{\frac{\partial \alpha_1}{\partial t}}{\frac{\partial n}{\partial \rho}} E \quad (11a)$$

$$\tilde{B} = B + \frac{\alpha_1 - \frac{\partial}{\partial t} \left(\frac{\partial t}{\partial \rho} \right)}{\frac{\partial n}{\partial \rho}} E \quad (11b)$$

$$\tilde{C} = C - \frac{\frac{\partial}{\partial t} \left(\frac{\partial n}{\partial \rho} \right)}{\frac{\partial n}{\partial \rho}} E \quad (11c)$$

$$\tilde{D} = D - \frac{\frac{\partial t}{\partial \rho}}{\frac{\partial n}{\partial \rho}} E. \quad (11d)$$

The third approximation is based upon the tangential derivative of the curvilinear Helmholtz equation, with terms involving third-order derivatives of the field ignored. The resulting expression for the mixed derivative, on the boundary, is

$$u_{tn} = -\frac{k^2}{\kappa} u_t - \frac{\kappa'}{\kappa} u_n.$$

The coefficients of the corresponding approximate RBC, (9), are

$$\tilde{A} = A \quad (12a)$$

$$\tilde{B} = B - \frac{k^2}{\kappa} E \quad (12b)$$

$$\tilde{C} = C - \frac{\kappa'}{\kappa} E \quad (12c)$$

$$\tilde{D} = D. \quad (12d)$$

The RBC obtained by Khebir, Ramahi, and Mittra has the same form as (9); however, their coefficients differ from each of the above. These differences arise from their use of approximations to u_ϕ and $u_{\phi\phi}$ which involve *only* tangential derivatives. Their coefficients are, in the current notation, ¶

$$\tilde{A} = \alpha_2^* \frac{\partial \rho}{\partial n} \quad (13a)$$

$$\tilde{B} = -\frac{\partial t}{\partial \rho} \frac{\partial \rho}{\partial n} \quad (13b)$$

$$\tilde{C} = -1 \quad (13c)$$

$$\tilde{D} = \beta_2^* \frac{\partial \rho}{\partial n} \left(\frac{\partial t}{\partial \phi} \right)^2. \quad (13d)$$

¶ In [5], the “second-order BT RBC” refers to (3) with coefficients, α_2^* and β_2^* , which are only $O(\rho^{-3})$ approximations to the exact coefficients, (4b). These RBCs were introduced in [11]. We see no practical reason to use the approximate coefficients in the present setting.

To conclude the discussion of the different RBCs, observe that each of the approximate RBCs reduces to the second-order BT RBC in the special case when the artificial boundary is a circle. The performance of these RBCs for different boundaries is examined in the next section.

IV. Comparison of Boundary Conditions

To evaluate the boundary conditions developed in the preceding section, we consider a test case involving a line source located at the origin. In particular, we examine the zero- and first-order terms of the Hankel function expansion of the solution to (1), i.e., $u_0 = H_0^{(2)}(k\rho)$ and $u_1 = e^{-j\phi} H_1^{(2)}(k\rho)$. Note that all derivatives of these solutions can be computed explicitly. This facilitates the comparison of the exact curvilinear representation of the second-order BT RBC (8) with the three approximate RBCs developed in Section III. The measure of error is defined to be the modulus of the pointwise difference between the approximate boundary condition and the exact normal derivative. The performance of these approximations on different artificial boundaries is shown in Figures 3–6.

It is important to stress that the objective of this investigation is to find a good approximation to (8), the exact curvilinear form of the BT RBC. We do not expect any of these conditions to improve upon the accuracy of the BT RBC.

In the subsequent comparisons, the boundary conditions are labeled as follows. The BT condition with exact evaluation of the mixed derivative term, (8), is denoted BT2(exact). The boundary condition developed by Khebir et al. [5], where both the mixed derivative and second normal derivative terms are absent, (9) with (13), is called BT2(KM approx.). The mixed derivative term in (8) could be dropped, (9) with (10), a boundary condition we call BT2(approx. u_{tn} with 0). The mixed derivative term could be approximated by differentiating the first-order BT condition with respect to t , resulting in BT2(approx. u_{tn} via BT1), which is the condition (9) with (11). Alternatively, u_{tn} could be formed by taking the derivative of the Helmholtz equation, (7). This results in third-order mixed derivatives, which are then discarded. This is (9) with (12), which is denoted BT2(approx. u_{tn} via PDE) in the figures.

Two different types of artificial boundaries are considered: elliptical and linear/circular or capped strip. The elliptical boundary, with a properly selected axial ratio, is conformable to a wide variety of scatterers. The capped strip boundary illustrates the performance when different types of curves are pieced together to form an artificial boundary. Three specific boundaries are considered: two ellipses of different axial ratios (Figures

3 and 4) and a capped strip (Figure 6). For each elliptical boundary, the absolute error in the normal derivative is evaluated for both u_0 and u_1 . In the capped strip example, the error is given for u_0 only. While these results are all obtained with $k = 2\pi$, similar performance is observed for a wide range of wave numbers. Recall that the goal of this exercise is to identify an RBC which closely approximates the BT condition, and not to minimize the absolute error over some portion of the domain.

The portion of an $(A \times B)$ elliptical boundary used for the computation of the error is shown in Figure 2. The source is located at $\rho = 0$. The abscissa for Figs. 3, 4 and 6 is the angle measured in degrees from the x -axis toward the y - axis. The errors for the exact BT condition and each approximation for elliptical boundaries with axial ratios of $(3\lambda \times 2\lambda)$ and $(3\lambda \times 0.5\lambda)$ are shown in Figures 3 and 4, respectively. Notice that the results are very similar for both u_0 and u_1 .

Two of the three approximations perform better than the BT2(KM approx.) condition. The BT2(approx. u_{tn} via BT1) approximation gives, on average, the best approximation over all points on the boundary and the simplest approximation. The BT2(approx. u_{tn} by 0) condition is surprisingly effective. The BT2(approx. u_{tn} via PDE) condition does not provide a good approximation, suggesting that the higher-order derivatives contain important information which should not be ignored.

Notice, in Figures 3 and 4, that the Bayliss-Turkel errors increase as the angle increases (in the first quadrant). This illustrates the fact that the Bayliss-Turkel RBCs are based on a far-field expansion. Each of the three proposed RBCs agrees with the original BT2(exact) RBC whenever $u_n = u_\rho$, i.e., at $\phi = 0$ and $\phi = \pi/2$. Another observation is that the peaks and dips in the error occur close to the inflection points of the curvature.

Figure 5 shows the capped strip boundary used to determine the normal derivative errors presented in Figure 6. Once again, the BT2(approx. u_{tn} via BT1) RBC performs best. The small jumps in the error coincide with the transition between the circular and planar sections of the boundary. The BT2(approx. u_{tn} via PDE) RBC cannot be used in this situation, as $\kappa = 0$.

Tests for different scenarios retain the general properties of the three examples shown here. The differences between the different boundary conditions decrease as the artificial boundary is moved closer (less than one wavelength) to the scatterer. This suggests that the approximate RBC (9) with (12) is an effective approximation to the curvilinear second-order BT RBC (8). It is expected that the approximate RBC (9) with (12) will permit

the use of smaller computational domains when numerically solving an exterior problem for the scalar Helmholtz equation than has been previously possible. A full finite element implementation of these ideas is in progress; the results will appear separately.

V. Conclusion

The extension of the Bayliss-Turkel radiation boundary condition to a general artificial boundary is presented. The presence of a mixed derivative term in this boundary condition makes it unsuitable for use in a variational method for the solution of the scalar Helmholtz equation. Three different approximations to the Bayliss-Turkel radiation boundary condition which are suitable for numerical computations are investigated. Of the three approaches considered, which were to neglect the cross term, to approximate it using the first order radiation condition, and to find an expression using the Helmholtz equation and neglect third order terms, the formation of the cross term using the radiation condition performed best. A wide range of boundaries and frequencies support this conclusion.

References

- [1] A. Bayliss and E. Turkel, "Radiation Boundary Conditions for Wave-Like Equations," *Comm. Pure Appl. Math.*, vol. 33, 1980, pp. 707–725.
- [2] A. Bayliss, M. Gunzburger and E. Turkel, "Boundary Conditions for the Numerical Solution of Elliptic Equations in Exterior Regions," *SIAM J. Appl. Math.*, vol. 42, no. 2, April, 1982, pp. 430–451.
- [3] T. G. Moore, J. G. Blaschak, A. Taflove, and G. A. Kriegsmann, "Theory and application of radiation boundary operators," *IEEE Trans. Antennas Propagat.*, vol. 36, Dec. 1988, pp. 1797-1812.
- [4] D. Givoli, "Non-reflecting boundary conditions," *J. Comp. Phys.*, vol. 94, 1991, pp. 1-29.
- [5] A. Khebir, O. Ramahi and R. Mittra, "An Efficient Partial Differential Equation Technique for Solving the Problem of Scattering by Objects of Arbitrary Shape," *Microwave and Optical Tech. Lett.*, vol. 2, no. 7, Jul. 1989, pp. 229–233.
- [6] R. Janaswamy, "2-D Radiation Boundary Conditions on an Arbitrary Outer Boundary," *Microwave and Optical Tech. Lett.*, vol. 5, no. 8, July 1992, pp. 393–395.
- [7] Y.-C. Ma, "A Note on the Radiation Boundary Conditions for the Helmholtz Equation," *IEEE Trans on Antennas Propagation*, vol. 39, no. 10, Oct. 1991, pp 1526-1530.
- [8] D. S. Jones and G. A. Kriegsmann, "Note on surface radiation conditions," *SIAM J. Appl. Math.*, vol. 50, Apr. 1990, pp. 559-568.
- [9] C. F. Lee, R. T. Shin, J. A. Kong, and B. J. McCartin, "Absorbing boundary conditions on circular and elliptical boundaries," *J. Electromagnetic Waves and Applic.*, vol. 4, no. 10, 1990, pp. 945-962.
- [10] S. N. Karp, "A convergent far field expansion for two dimensional radiation functions," *Comm. Pure and Applied Math.*, vol. 14, 1961, pp. 427-434.
- [11] O. Ramahi and R. Mittra in M. A. Morgan, *Finite Element and Finite Difference Methods in Electromagnetic Scattering*, PIER 2, Elsevier, 1990, Section 4.4, pp. 143–149.

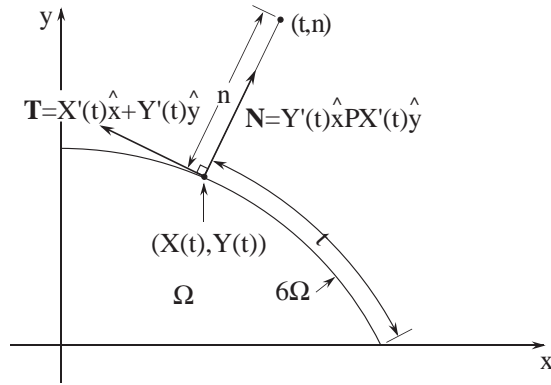


Figure 1. Cartesian, polar, and normal/tangential coordinate systems.

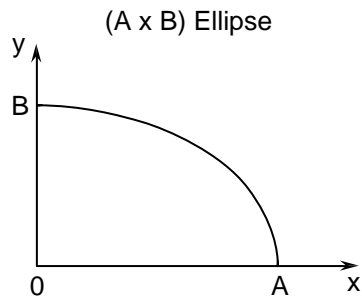


Figure 2. The first quadrant of an $(A \times B)$ elliptical boundary.

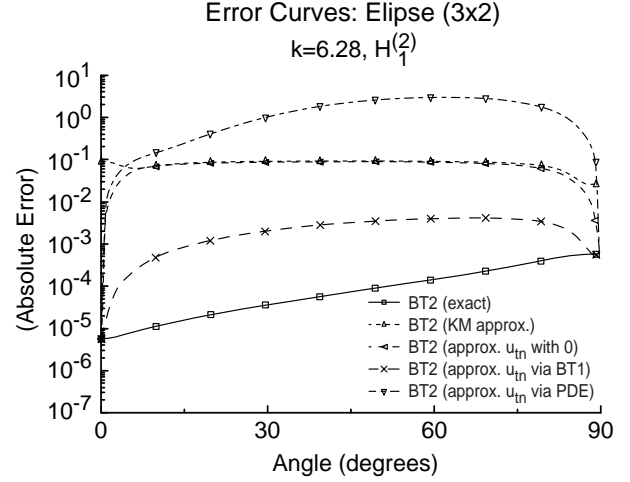
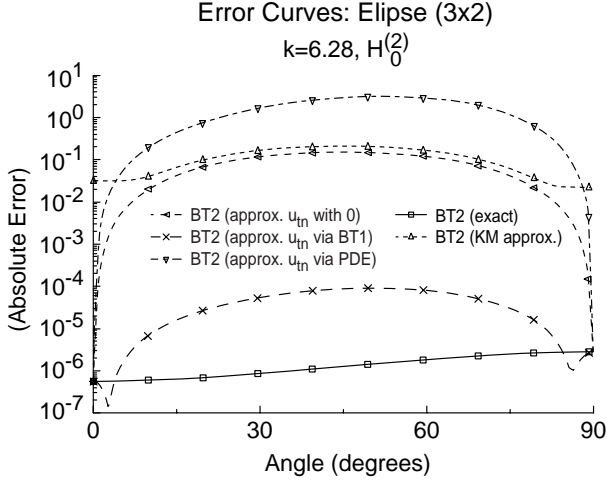


Figure 3. Comparison of RBCs for the scalar Helmholtz equation with $k = 2\pi$ when the artificial boundary is a $(3\lambda \times 2\lambda)$ ellipse. The absolute error is the modulus of the difference between the exact and approximate values of the normal derivatives for (a) $u_0 = H_0^{(2)}(k\rho)$ and (b) $u_1 = e^{-j\phi} H_1^{(2)}(k\rho)$.

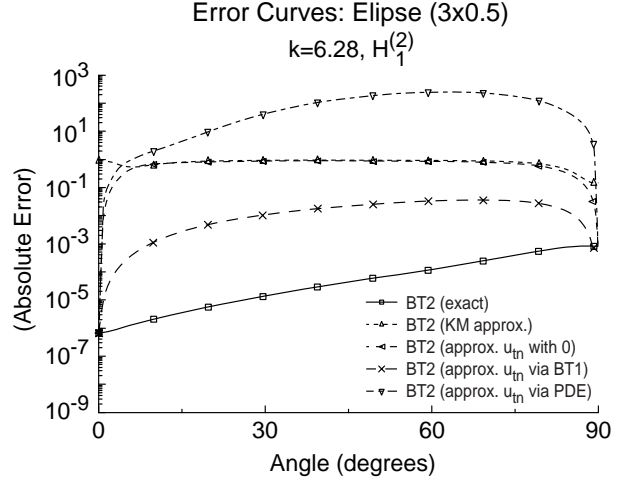
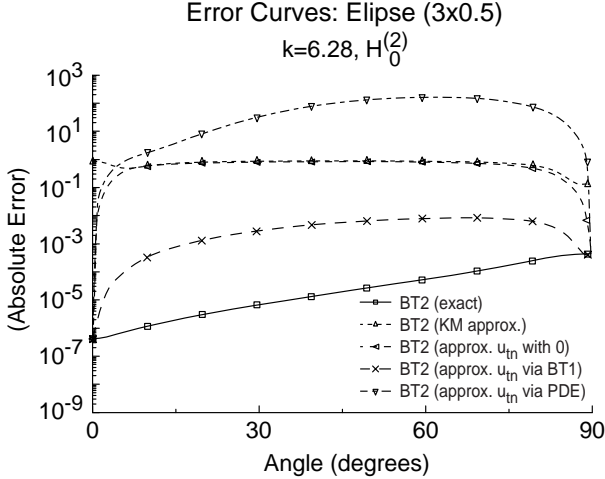


Figure 4. Comparison of RBCs for the scalar Helmholtz equation with $k = 2\pi$ when the artificial boundary is a $(3\lambda \times 0.5\lambda)$ ellipse. The absolute error is the modulus of the difference between the exact and approximate values of the normal derivatives for (a) $u_0 = H_0^{(2)}(k\rho)$ and (b) $u_1 = e^{-j\phi} H_1^{(2)}(k\rho)$.

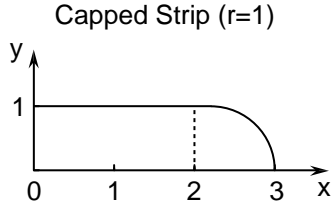


Figure 5. The first quadrant of the capped strip boundary with radius 1.

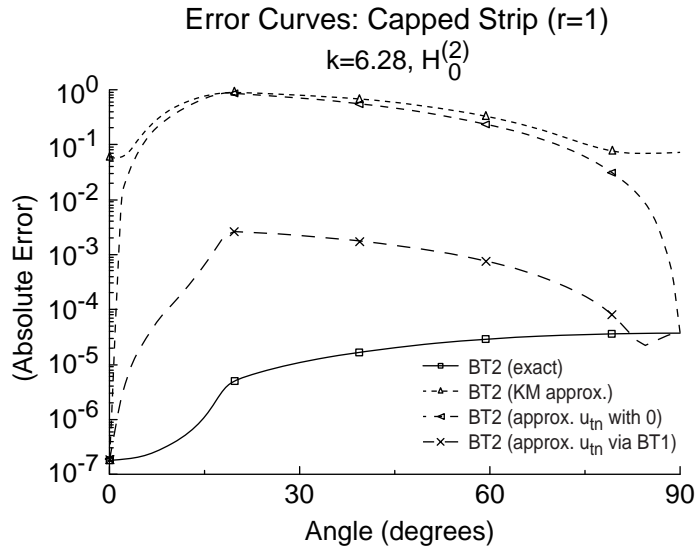


Figure 6. Comparison of RBCs for the scalar Helmholtz equation with $k = 2\pi$ when the artificial boundary is a capped strip with radius 1. The absolute error is the modulus of the difference between the exact and approximate values of the normal derivatives for $u_0 = H_0^{(2)}(k\rho)$.